Zhang *et al.*
Journal of Engineering and Applied Science (2023) 70:156
https://doi.org/10.1186/s44147-023-00321-6

Journal of Engineering and Applied Science

RESEARCH Open Access

Harmonic control method for multiple driving cycles of EMU based on improved C-type filter

Haigang Zhang[1*], Haoqiang Zhou[1], Decheng Zhao[1], Song Zeng[1], Zizhuo Wang[1], Jianpeng Zhu[1], Bulai Wang[1] and Jinbai Zou[1]

*Correspondence:
haigangzhang142@163.com

[1] School of Rail Transit of Shanghai Institute of Technology, Shanghai 201418, China

Abstract

For traction substation (TS), the harmonic current spectrum distribution of the left and right power supply sections has a large difference under different EMU operating conditions. This phenomenon will further affect the harmonic distribution of the entire traction power supply system and has the risk of harmonic distortion. At the same time, it may also cause interference to the communication line. In this paper, the transient direct current control technology is used to realize the converter of EMU, and then the TS side harmonic model under regenerative braking condition is realized. The harmonic problem, control process, and negative sequence problem caused by locomotive traction braking on the TS side under various working conditions are analyzed in detail. After connecting the C-type filter to the traction network side of the system, the THD (total harmonic distortion) is within the standard range, while the negative sequence problem of the system has worsened. Therefore, the parameters of the filter were optimized to improve both harmonics and negative sequence problems by combining the negative sequence characteristics under various operating conditions. The results show that the improved treatment can effectively control the harmonic problem.

Keywords: Regenerative braking, Harmonic control, Multi-condition analysis, Negative sequence analysis

Introduction

With the improvement of the construction of eight vertical and eight horizontal railway lines in China, the problem of harmonic pollution in the traction power supply system (TPSS) has gradually increased, and its causes and related calculation methods have been widely studied [1–4]. The negative sequence current can cause power system generator rotor overheating, vibration, causing relay protection device malfunction and a series of problems. To a certain extent, these factors bring risks to the safe and stable operation of distribution network and EMU [5]. At present, there are many researches on harmonic and negative sequence current at home and abroad, but the completeness of the simulation system is insufficient. That is, the load of the EMU is equivalent to

the resistive load connected to TPSS. Although the negative sequence law is reflected, it lacks the completeness of modeling [6–8]. C-type filter has been used in power system for a long time, but the harmonic spectrum of high-speed trains has random dynamic characteristics due to the variety of high-speed trains and frequent operating conditions, and the movement of large harmonic source immediately affects the system harmonic transmission characteristics [9]. Therefore, the general C-type filter is difficult to completely compensate harmonics.

Although the existing passive compensation scheme is still within the acceptable cost range and the effect is considerable, a single compensation is difficult to cope with the high load fluctuation of TPSS. Therefore, some scholars have studied the application of static var compensator (SVC) [10, 11] and static synchronous compensator (STATCOM) [12] in power supply system of electrified railway. However, after injecting reactive power, such devices often cannot simultaneously adjust current imbalance and harmonics. Existing power quality compensators can operate in full compensation (FC) mode, such as traditional RPC (railway static power conditioner) [13–16], but the disadvantage of these regulating units is that they generally have relatively high DC voltage component and power loss, without cost advantage. Therefore, some scholars have proposed related schemes: (1) adopt variable control and partial compensation strategy (PC) [17, 18] in the control method, and (2) at the level of physical equipment, use low-rated secondary equipment to reduce costs, such as SVC and passive LC branch [19, 20]. In addition, the C-type filter often acts on the attenuation of higher harmonics, because the active loss of the filter at the fundamental frequency is negligible [21]. Some of the previous design methods are mostly from the perspective of resonance damping rather than from the perspective of filtering performance [22, 23]. In Reference [24], a C-type filter was designed for the arc furnace system at the second harmonic. However, higher parameter tuning is suitable for TPSS.

In this paper, the above problems, through the self-built traction power supply system regenerative braking model, more abundant train operation conditions are obtained, and the harmonics and negative sequence problems caused by locomotive traction braking on the TS side under various working conditions are analyzed in detail. From the perspective of multiple working conditions, the C-type filter parameters are optimized for harmonic control, which is more in line with the engineering practice of TPSS.

The harmonic problems of TPSS

The locomotive is main source of harmonics of TPSS, and the traction network is a complex power supply network composed of multiple irregular cables such as contact lines, load-bearing cables, positive feeders, and rails. There is a large distributed capacitance and inductance between the power supply lines. When the distributed capacitance and inductance are impedance matched with other equipment of the system at a certain frequency, the system resonance point will be formed. When the output current by the EMU contains harmonics near the resonance point, high-order harmonic resonance overvoltage will be generated. When taking single-row α-braking as an example, the harmonic distribution of vehicle-grid coupling is shown in Fig. 1.

Figure 1 shows the interaction mechanism of the three, and the main difference is 5 to 30 harmonics and 70 to 80 harmonics. The harmonic current content near the

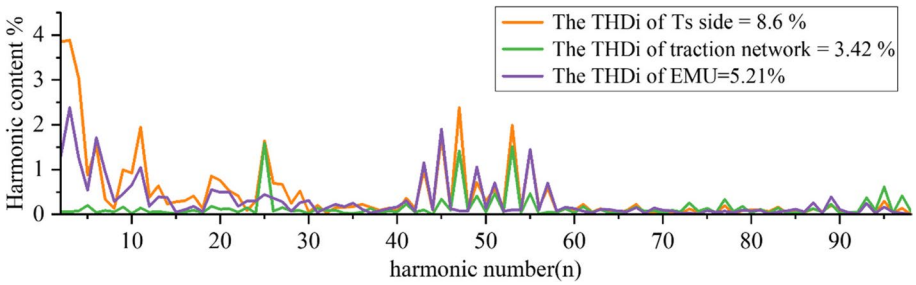

Fig. 1 Harmonic distribution of EMU, traction network, and TS side

27th injected by the EMU is relatively low, indicating that the higher harmonic voltage near the 27th may be due to the resonance point near the system, resulting in resonance amplification, thus presenting the distribution of harmonics before and after the TS transformation in Fig. 1. The negative sequence fluctuation caused by harmonic impedance in filtering cannot be ignored. Therefore, in the design of harmonic control scheme, the influence of many aspects and working conditions should be considered comprehensively, and the filtering effect should be defined in combination with the harmonic standard of TS side in Table 1.

Methods of power improvement in TPSS

Locomotive transient direct current control technology

In this paper, the transient current local control scheme is used to control the signal of the converter. The main steps of the scheme are shown in formula 1. The control logic is shown in Fig. 2b.

Table 1 Harmonic standards for TS side [25]

Voltage (kV)	THD (%)	Number of harmonics THD (%)	
		Odd harmonic	Even harmonics
0.38	5	4	2
6.10	4	3.2	1.6
66.35	3	2.4	1.2
110/220	2	1.6	0.8

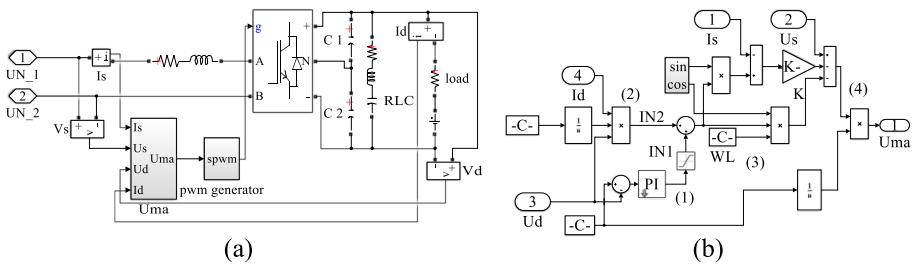

Fig. 2 **a** PWM control logic diagram of three-level converter. **b** Design of converter

$$\begin{cases} I_N^* = I_d U_d / U_n + K_p(U_d^* - U_d) + 1/T_i \int (U_d^* - U_d) \\ u_{ab}(t) = u_N(t) - \omega L I_N^* \cos\ \omega t - R_N I_N^* \sin\ \omega t - K\left[I_N^* \sin\ \omega t - i_N(t)\right] \end{cases} \tag{1}$$

In Formula (1), U_d is the actual voltage of the intermediate DC circuit, $i_N(t)$ is the actual input current of the TS side, and U_d^* and I_N^* are the given values of the two respectively; I_d is the current corresponding to DC circuit. ω_0 represents the fundamental angular frequency of the input signal. U_s, I_s, I_d, and U_d are the input signals of the control system The proportional and integral constants include T_i, G_2, and T_i.

When $U_d = U_d^*$, error $\zeta = 0$, PI regulation keeps constant output, rectifier DC side, and AC side power balance:

When $U_d < U_d^*$, error $\zeta > 0$, the inner-loop current of PI regulation output will increase, and the input current and power of rectifier will increase, so the inner-loop current reflects the change of required power.

The converter calculates the modulation signal $u_{ab}(t)$ according to the collected U_d, I_d, U_S, and I_S and the transient current control algorithm described above. In Fig. 2b, position ① generates I_{N1} through PI control, position ② generates I_{N2}, ③ corresponds to output I_N^*, and ④ corresponds to output $u_{ab}(t)\prime$ before normalization. Because the amplitude of $u_{ab}(t)\prime$ modulation signal should be less than the triangular wave, the normalized output is divided by the given voltage value U_d^*.

This locomotive model refers to the CRH2 circuit to establish a simulation model. Due to the emphasis on the grid-side current and voltage, the inverter and its control are simplified as the load of the converter. The train simulation model is built according to the PWM control logic in Fig. 2a. The model includes the traction main transformer, three-level bridge circuit, modulation wave generation module, PWM control module, intermediate DC voltage link, secondary filtering, and inverter load. When simulating the regenerative braking, a DC voltage source is connected in series at the load.

The transient current control is simple, and the generated PWM is a five-level voltage level control signal $(U_d, U_d/2, 0, -U_d/2, -U_d)$, This method can simply and efficiently filter out the harmonic current generated by the secondary side equipment. Its dynamic response is fast, and only a small voltage ripple is generated on the DC side.

Negative order imbalance problem

The unbalance degree is positively correlated with the negative sequence current value. The three-phase voltage and current of the power supply side of the system are expressed by $\left[\ \dot{U}_A\ \ \dot{U}_B\ \ \dot{U}_C\ \right]$ and $\left[\ \dot{I}_A\ \ \dot{I}_B\ \ \dot{I}_C\ \right]$, respectively. The corresponding locomotive load side current and terminal voltage are expressed as I_P and U_P, $P = 1, 2, \cdots n. \cdot U_A$ as a reference phasor is as follows:

$$\left[\ \dot{U}_A\ \ \dot{U}_B\ \ \dot{U}_C\ \right]^T = \left[\ 1\ \ a^2\ \ a\ \right]^T U_A \tag{2}$$

$$\dot{U}_P = U_P e^{-j\varphi P} = \sqrt{3} K_P U_A e^{-j\varphi P}, \dot{I}_P = \dot{I}_P e^{-j(\varphi P + \phi P)} \tag{3}$$

$$K_P = U_P / \left(\sqrt{3} U_A\right) \tag{4}$$

In the formula (2), $a = e^{j120^\circ} = -0.5 + \sqrt{3}/2j$ denotes unit vector operator, $\dot{U}_P$ lags phase angle φ_P than $\dot{U}_A$, and $\dot{I}_P$ lags power factor angle ϕ_P than $\dot{U}_P$. Zero sequence current does not appear on the system side under independent operating conditions, so the three-phase current generated by I_P is collinear with I_P and satisfies $I_{AP} + I_{BP} + I_{CP} = 0$ and then comes to the conservation principle formula.

$$\begin{aligned} &\dot{U}_A \times \dot{I}_{AP} + U_B \times \dot{I}_{BP} + \dot{U}_C \times \dot{I}_{CP} = \dot{U}_P \times \dot{I}_P \\ &P = 1, 2, \cdots, n \end{aligned} \tag{5}$$

The three-phase current expression can be obtained from the symmetrical component method and superposition principle described in Reference [26]:

$$\begin{bmatrix} \dot{I}_{AP} \\ \dot{I}_{BP} \\ \dot{I}_{CP} \end{bmatrix} - \frac{1}{\sqrt{3}} \begin{bmatrix} 1 & 1 & 1 \\ 1 & a & a^2 \\ 1 & a^2 & a \end{bmatrix} \begin{bmatrix} 0 \\ \sum_{P=1}^{n} K_P \dot{I}_P e^{-j\varphi P} \\ \sum_{P=1}^{n} K_P \dot{I}_P e^{j\varphi P} \end{bmatrix} \tag{6}$$

The expressions of positive sequence and negative sequence current and the unbalance degree of negative sequence current are obtained from Formulas 7 and 8.

$$\begin{cases} I^+ = \frac{1}{\sqrt{3}} \sum_{P=1}^{n} K_P \dot{I}_P e^{-j\varphi P} \\ I^- = \frac{1}{\sqrt{3}} \sum_{P=1}^{n} K_P \dot{I}_P e^{-j(2\varphi P + \phi P)} \end{cases} \tag{7}$$

$$\varepsilon = \left| \frac{I^+}{I^-} \right| \times 100\% \tag{8}$$

Among them, I^+ and I^- are positive sequence and negative sequence current components respectively, and the unbalance degree of negative sequence current is expressed by ε. The change of three-phase unbalance can be accurately reflected by the characteristics of negative sequence current. The negative sequence will be represented later by I^-.

C-type filter and its parameter optimization design

Harmonic control schemes include active APF (active power filter) and passive PPF (passive polyphase filter) filtering, and there is no filter scheme such as optimizing system parameter configuration, which affects harmonic distribution [27]. Because TPSS is a typical dynamic harmonic system, APF which can realize dynamic range filtering should be the most suitable scheme. But in terms of cost, the input cost of APF is higher. In addition, due to the comprehensive influence of TPSS topology and the number of distribution network equipment in China, the harmonic problem is relatively light. PPF has frequency modulation characteristics. Therefore, PPF is widely used in most TPSS harmonic control. In terms of connection mode, PPF has two combinations of series and parallel. Parallel installation is more convenient, compared with the series form, and its impact on the system is smaller. The structure of parallel filter is shown in Fig. 3.

Where (a) single tuning, (b) 1-order, (c) 2-order, (d) 3-order and (e) C-type filters. The C-type filter has the characteristics of frequency scanning. The TPSS harmonic characteristics in Fig. 1 show that the power supply system has obvious resonance frequency.

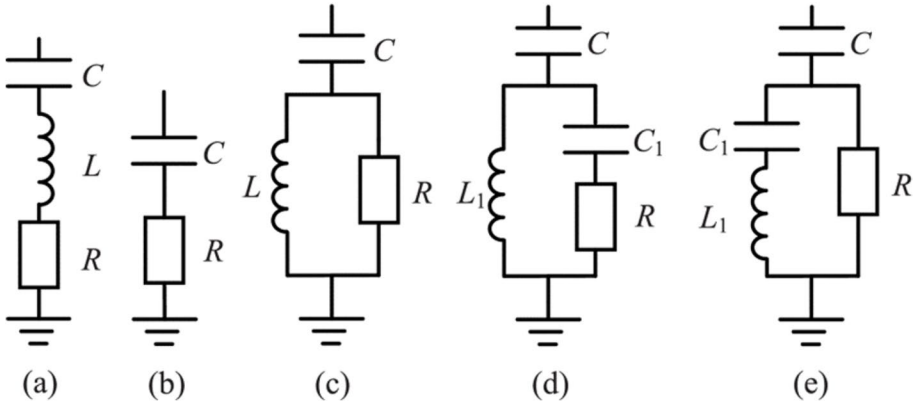

Fig. 3 Structure of parallel harmonic filter

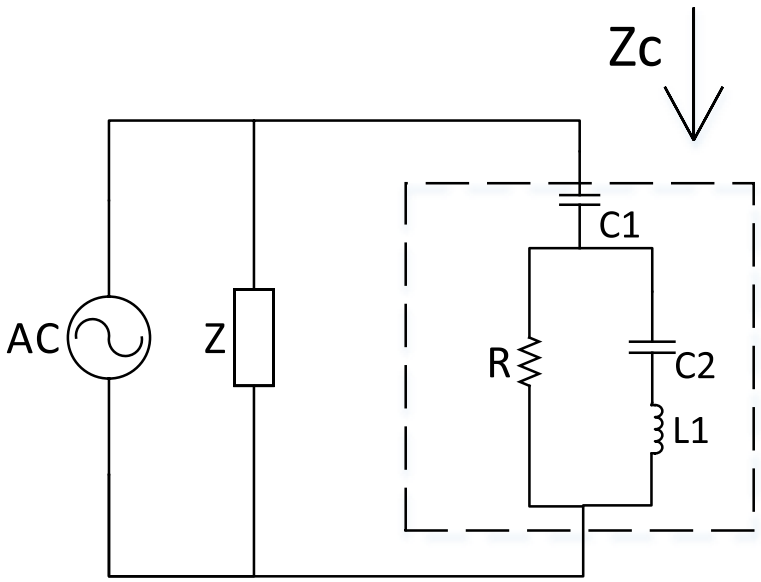

Fig. 4 Adding the equivalent circuit of the filter

In this paper, the C-type filter is arranged between the T contact wire and the ground wire of the traction substation for frequency scanning. The traction power supply system can be equivalent to the equivalent circuit shown in Fig. 4.

The impedance Z_c of the C-type filter can be expressed as follows:

$$\begin{aligned} &Z_{\mathrm{c}} = R\frac{(X_L - X_{C2})^2}{R^2 + (X_L - X_{C2})^2} + j\left[\frac{R^2(X_L - X_{C2})^2}{R^2 + (X_L - X_{C2})^2} - X_{C1}\right] \\ &X_L = n\omega_1 L, \\ &X_{C1} = 1/(n\omega_1 C_1) \\ &X_{C2} = 1/(n\omega_1 C_2) \end{aligned} \tag{9}$$

where X_L, X_{C1}, X_{C2}, and R correspond to the impedance values of the inductor L, the capacitor C1 and C2, and the parallel resistor R of the C-type high-pass filter, respectively; here, n denotes the harmonic order, and ω_1 denotes the fundamental angular

frequency. The filter resistance frequency characteristic equation is expressed as Formula 10:

$$\begin{aligned} &\frac{|Z_c|}{R} = \sqrt{X_1 + X_2} \\ &X_1 = \frac{1}{(N\omega_1 C_1 R)^2} \\ &X_2 = \frac{\left((n\omega_1)^2 LC_2 - 1\right) \times \left((n\omega_1)^2 LC_2 - 1 - 2C_1/C_1\right)}{\left((n\omega_1)^2 LC_2 - 1\right)^2 + (n\omega_1 C_2 R)^2} \end{aligned} \tag{10}$$

For the convenience of representation, let the sub-terms of the square sum of impedance modulus be X_1 and X_2, respectively.

Simulation analysis and example verification

Establishment of locomotive model

The CRH2 (CRH380AL) train circuit simulation model is built with reference to Fig. 2 of the locomotive model. The inverter and its control are simplified and equivalent to the load of the converter, which is replaced by branch load. The model includes traction transformer, rectifier, modulation wave generator, PWM controller, intermediate DC voltage link, secondary filter, and inverter load. When simulating regenerative braking conditions, a DC voltage source is connected in series at load.

The CRH2 EMU has two adjacent motor vehicles as the basic unit. The whole vehicle has two units. One basic unit includes a main transformer and two traction converters. EMU system parameters of CRH2 are shown in Table 2.

Figure 5 shows the model of the EMU; the receiving part of the catenary is temporarily replaced by 25-kV AC power supply.

The carrier frequency of the converter equal to 1250 Hz, the equivalent load resistance load of the inverter part of the converter equal to 6.89 Ω, and the regenerative braking voltage level equal to 5000 V.

Locomotive harmonic source model simulation

The rated traction condition ($U_N = 1500V, P = 5184kW$) of the locomotive is tested. The model carrier modulation results are shown in Fig. 6a and b.

It can be found that in the control signals of the simulation model in Fig. 7, the phase difference between the carrier and modulating waveforms of phase A and phase B is 180°, and the phases of the modulating waveform and the carrier waveform meet the requirements. The locomotive side voltage and current and their phase relationship are

Table 2 EMU model simulation parameters

Equipment	Parameter
Two primary windings of main transformer	25 kV, 3060 kVA
Four secondary windings of main transformer	1500 V, 1285 kVA
Traction converter input	1285 kVA/1500 V/857 A
Traction converter output	1296 kW (3000 V, 432 A)
Traction transformer side resistance inductance	$R = 0.22\ \Omega$, $L = 1.18$ mH
Intermediate support capacitance	1245 uF
PI parameters of UMA module	Kp = 0.2; Ki = 15

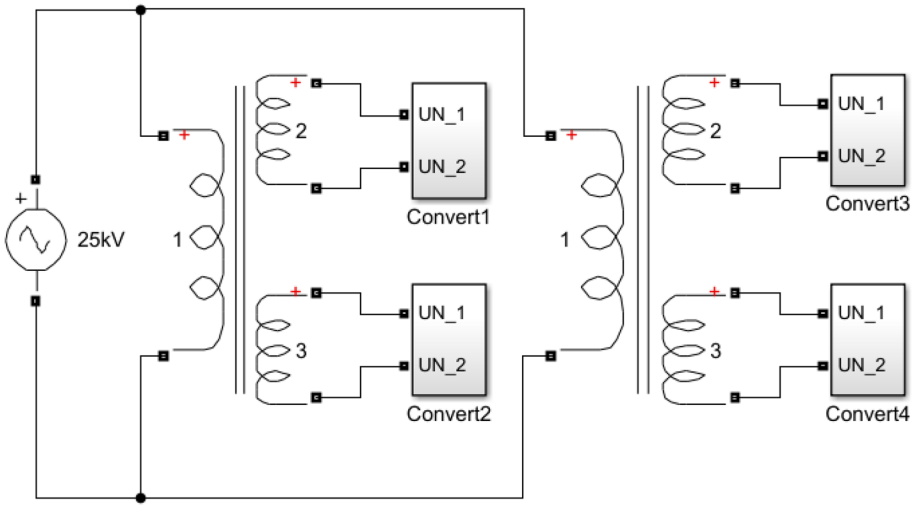

Fig. 5 Model design of EMU. **a** Phase A modulation wave and carrier wave. **b** Phase B modulation wave and carrier wave

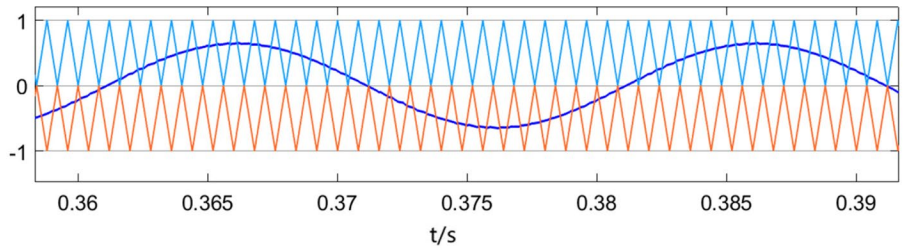

(a) Phase A modulation wave and carrier wave.

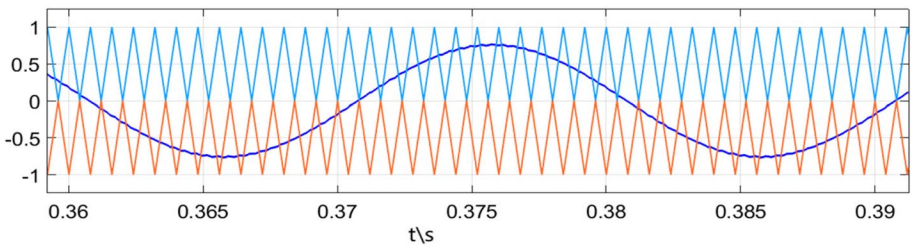

(b) Phase B modulation wave and carrier wave.

Fig. 6 Modulation waveform of locomotive converter

analyzed under the traction state and regenerative braking state respectively, as shown in Fig. 7, where Fig. 7c and d represents the measured and simulated waveforms of three-phase voltage in TS, and the data are taken from the Harbin-Dalian line railway, and it can be concluded that the model reflects the real operation situation. Then, the harmonic content of the TS side current is analyzed by double FFT harmonic analysis method, as shown in Fig. 8.

Under the traction condition shown in Fig. 8a, the current harmonic distribution trend of CRH2 EMU is roughly the same as the voltage level. The AC input terminal voltage is an equivalent sine wave of five-level $(U_d, U_d/2, 0, -U_d/2, -U_d)$ pulse ,

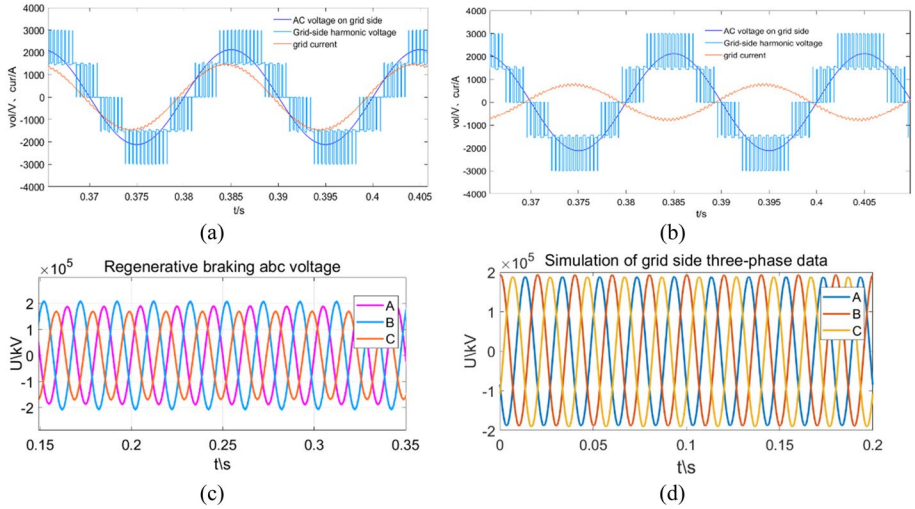

Fig. 7 Converter control voltage level under traction (**a**) and braking (**b**) condition, measured (**c**) and simulated (**d**) waveforms

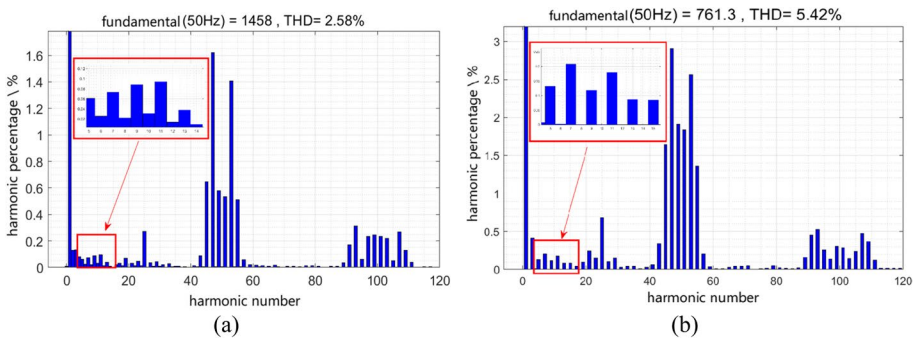

Fig. 8 Harmonic distribution under traction (**a**) and braking (**b**) condition

and the current also conforms. Voltage and current reverse phase when train brakes, which is in line with the actual working condition. The grid-side FFT analysis results of the two conditions show that the current has even harmonic doping under traction conditions, while the regenerative braking condition in Fig. 8b has only odd harmonics.

The high-order harmonics are roughly distributed at the integer multiple of ω_0, while the low-order harmonics are mainly concentrated in 5, 7, ..., 13 times. The carrier ratio $n = 1250/50 = 25$, so the harmonics are distributed in 50 ± 7(odd) and 100 ± 7(odd) times. This is due to the harmonic distribution caused by the harmonics generated by some nonlinear equipment in the locomotive during operation. Under the rated load, the harmonic distortion rate is in the normal range. When regenerative braking, the grid-side voltage and current are reversed, and the converter acts as an inverter to output negative power in reverse. It is verified that the harmonic content and voltage level in the above waveform are synchronized with the theoretical analysis, and the model can be further analyzed.

Table 3 Simulation parameters of TPSS

Parameters	Value
Three-phase system voltage/kV	220
Traction substation capacity/MW	40
Traction substation transformer ratio	220:27.5
AT capacity MW	40
Simulation duration/s	0.3

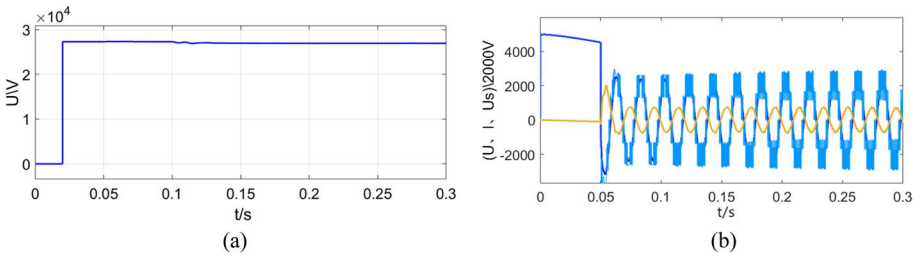

Fig. 9 The voltage of AT (**a**) and locomotive regenerative braking (**b**)

Harmonic characteristics and negative sequence analysis of TPSS under multiple conditions

The paper builds a TPSS model to simulate various operating conditions of CRH2 (CRH380AL) trains running in the TPSS. Because when the train runs, as a dynamic large-scale load body, it is not uncommon for two vehicles to run simultaneously on the traction network. It is necessary to analyze I^- and harmonics of each operating condition. Considering the line loss on the low-voltage side of the traction network during locomotive operation, the locomotive power supply voltage will be increased by 10% for voltage level compensation, that is, $25 \times (1 + 10\%) = 27.5$ kV. Combined with the electrical parameters of a domestic traction substation, the parameters of TPSS are shown in Table 3.

Traction substation adopts V/x wiring, namely the primary side connected with AB and BC phase and secondary side neutral grounding. The traction network supplies power for AT. By setting the circuit breaker switch, simulate the train transit. In the absence of train transit, the line is empty, and I^- is only generated by the TPSS. Next, the harmonic and negative sequence conditions of different working conditions are analyzed in detail, and the observation range is 0–0.3 s. First, ensure that the AT voltage is 27.5 kV level in Fig. 9a, and the train runs normally in the TPSS.

Under the condition of regenerative braking, Fig. 9b shows the train operation control waveform. In order to facilitate observation of train braking process, the access time is set to 0.05 s. The waveform shows that the control voltage is maintained near the rated 3000 V, and the train runs stably in the TPSS. Combined with the parallel harmonic filter in Fig. 3 and the TPSS built above, six types of locomotive working conditions are designed in Table 4 to analyze I^- and harmonics on the grid side.

Next, combined with the above conditions, by controlling the locomotive running state simulation, to case 1 as an example: double traction, the uplink power supply

Table 4 Description of six working conditions

Condition category	Condition description
(1) Double-row traction	Bilateral power supply arms are traction operation
(2) α Traction-β braking	Left traction, right braking
(3) Double-row braking	Bilateral power supply arms are braking operation
(4) α braking-β traction	Left braking, right traction
(5) Single-row braking	Brake only on one side, no car on the other
(6) Single-row traction	Traction only on one side, no car on the other

arm has a train through, the downlink power supply arm has a train through, and the state is traction operation. The resulting harmonic distribution is shown in Fig. 10.

It can be concluded from Fig. 11 that the 25th harmonic content gradually increases with the time of EMU access, which is due to the converter carrier modulation of 1250 Hz. In order to more specifically describe the harmonic data under multi-cycle conditions, the stable harmonics at 0.22 s are taken, and the harmonic content of each working condition is compared horizontally as follows.

It can be seen from Fig. 12 that under all working conditions, the harmonic characteristics generally conform to the harmonic distribution of the locomotive harmonic source coupling traction network in Fig. 1, and the high-frequency harmonics of most working conditions are concentrated near 50 times. Under the braking condition of single train, the high-frequency harmonic current near 80–90th harmonics is obviously amplified. The maximum difference between the double-row traction condition and the double-row braking condition is about 27 harmonics, indicating that the braking condition has a greater impact on the traction network.

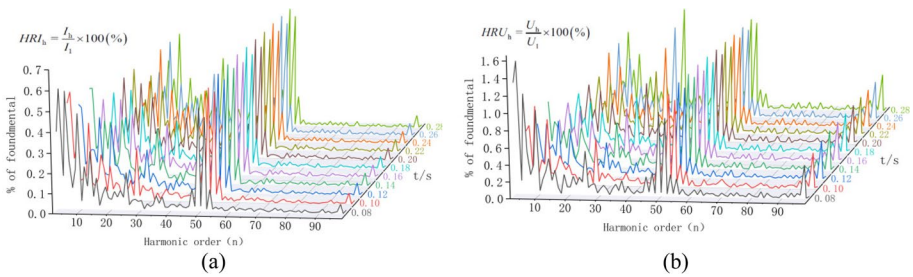

Fig. 10 The harmonic distribution of current (**a**) and voltage (**b**)

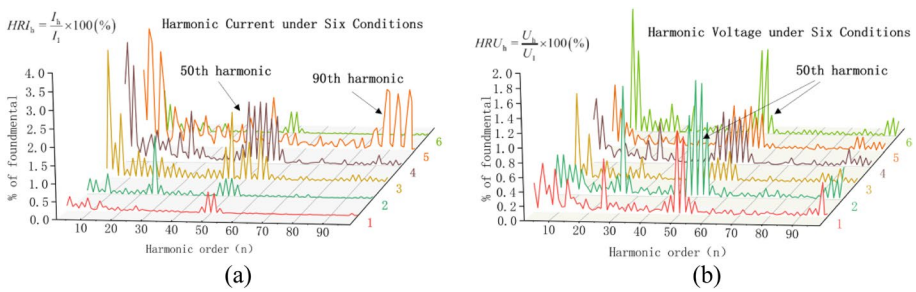

Fig. 11 The harmonic distribution of current (**a**) and voltage (**b**) under various operating conditions

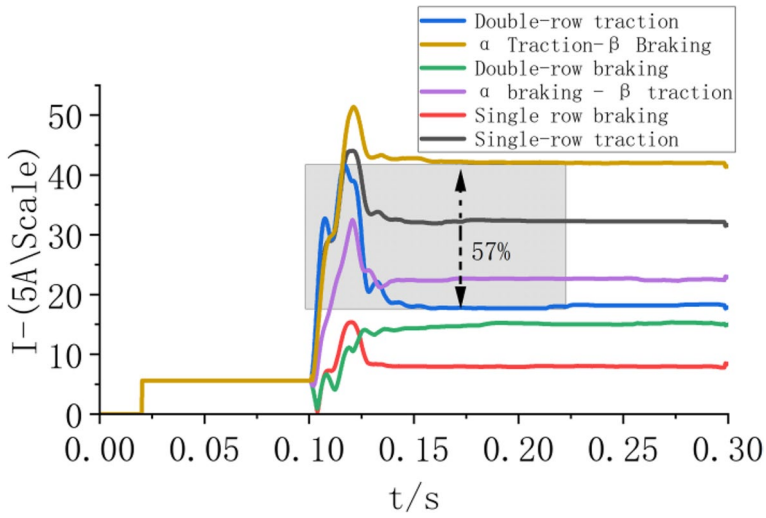

Fig. 12 The negative sequence characteristic waveform under six conditions

Table 5 TS side harmonic and I⁻ level under different conditions

Condition category	I⁻ values		THDi/THDu	
	Peak value	Stable value	When accessing	After stabilization
1	41.2	17.5	1.34/3.31	1.21/2.62
2	51.2	41.9	4.58/2.34	4.13/2.91
3	15.7	15.1	6.68/2.24	5.63/1.68
4	32.1	22.9	5.01/1.84	7.12/2.97
5	15.3	8.1	4.83/1.91	5.11/2.12
6	44.1	32.2	1.61/2.81	1.85/3.13

The above harmonic characteristics can be used to study the differences between different working conditions. The results are shown in Table 5.

From Table 5, under the traction condition, the negative sequence fluctuation is the largest, and the negative sequence level is the lowest when the running conditions of the bilateral locomotives are different. On the whole, it shows the characteristics of high negative sequence in traction condition and low negative sequence in braking condition. Especially in the double-row traction condition, the negative sequence fluctuation is very large, and the drop is as high as 57%. The harmonic content also shows a clear distinction. For example, when the α power supply arm has a braking condition, the harmonic content is significantly higher than other working conditions, and the harmonic content is the highest when the double row brakes. The negative sequence characteristic waveforms under six conditions are shown in Figs. 12 and 13.

The trend of total harmonic content of current and voltage under six operating conditions is shown in Fig. 13b and c. Experiments show that the harmonic content under various working conditions has a good discrimination, and when the braking condition is dominant, the THDi and THDu harmonic content increases exponentially compared with the traction condition. The results meet the requirements of feature classification and can be used for further feature recognition.

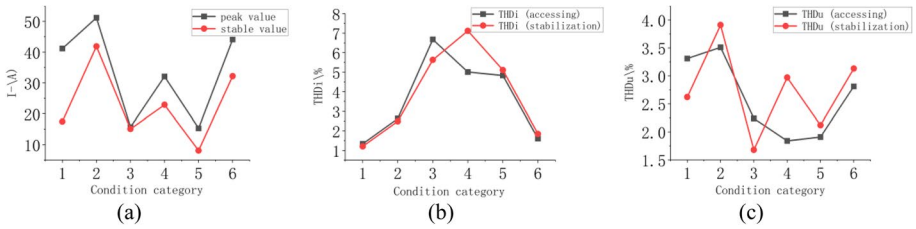

Fig. 13 **a** Negative sequence trend. **b** Harmonic content of current. **c** Harmonic content of voltage

Parameter adaptive experiment of C-type filter for six working conditions

Next, for the above harmonic problems, C-type filter with adaptive parameter method. Parameter settings are as follows:

The ordinary parameter is as follows: C1 = 1.014 uF, C2 = 540 uF, L = 18.4 Mh, and R = 100 Ω. According to the characteristics of multi-condition preset optimization parameter range, C2 = 540~1000 uF, and r = 100~300 Ω; due to many working conditions, just show one of working conditions is taken as an example here. Taking working condition 2 as an example, the C-type filter and the optimized filtering effect are shown in Fig. 14. In order to further study the filtering effect, the harmonic filtering effect of the AT voltage is evaluated. The experimental results are shown in Figs. 15 and 16.

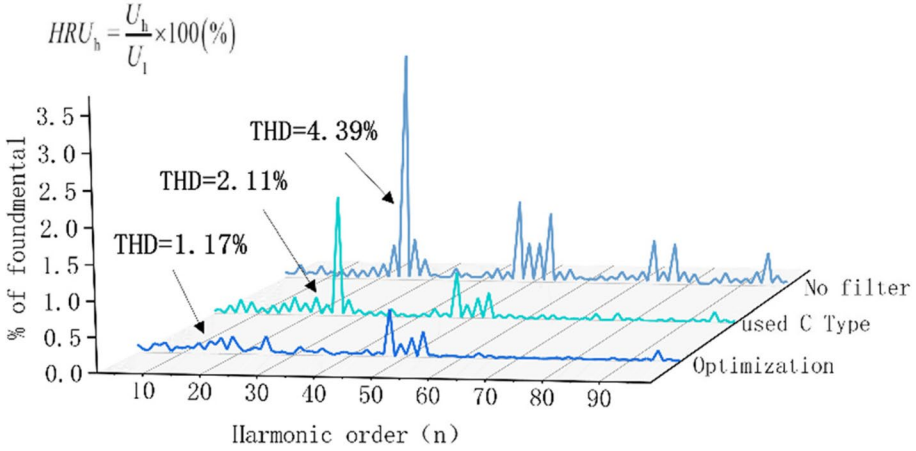

Fig. 14 Harmonic content of traction network voltage

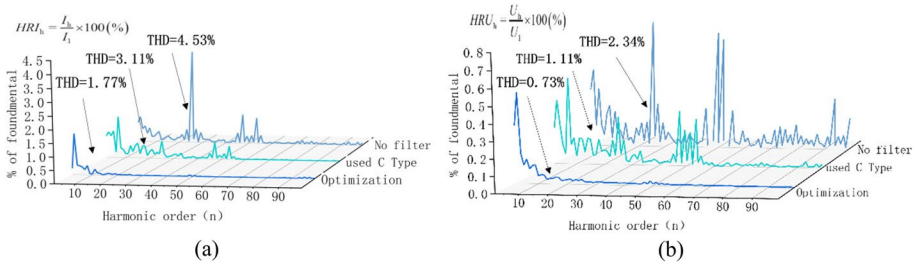

Fig. 15 Harmonic content of TS side current (**a**) and voltage (**b**)

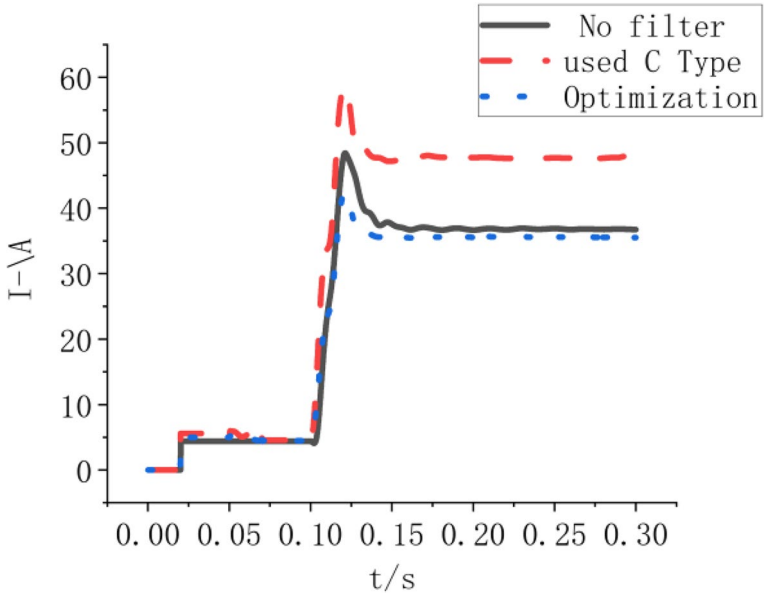

Fig. 16 Comparison of negative sequence characteristic waveforms before and after filtering

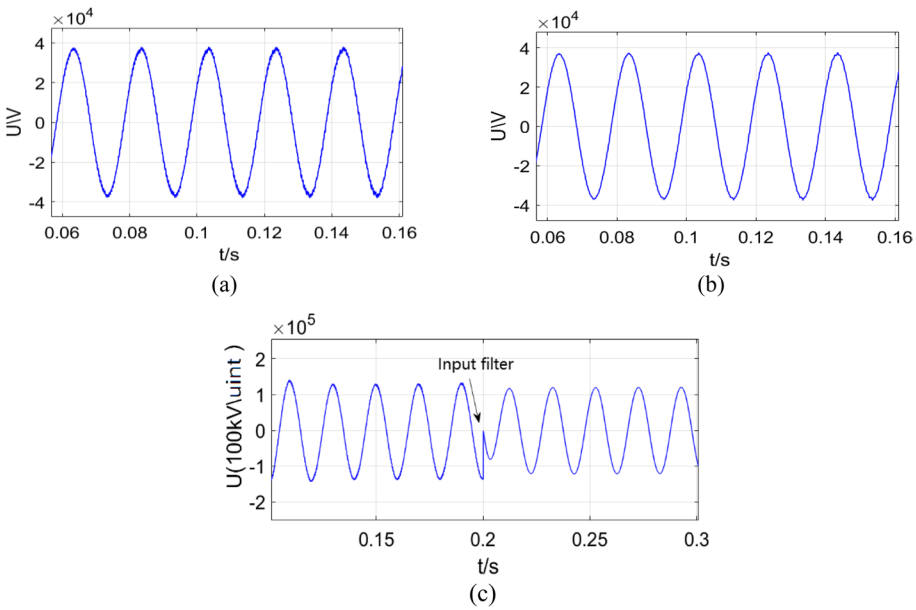

Fig. 17 Traction network (**a**, **b**) and grid voltage waveform before and after filtering (**c**)

Results and discussion

The results show that the filtering scheme eliminates most of the harmonics. The THDi of the TS side is reduced from 4.53 to 3.11%. The THDu is reduced from 2.34 to 1.11%, and the THDu of the traction network is reduced from 4.39 to 2.11 %. Although most of the high-frequency components are filtered out after C-type filtering, the harmonic components of 23.25 and other harmonics are still outstanding. The negative sequence component has an increasing trend, so the final negative sequence is adjusted by optimizing the capacitor capacity and resistance value. Figure 17 shows

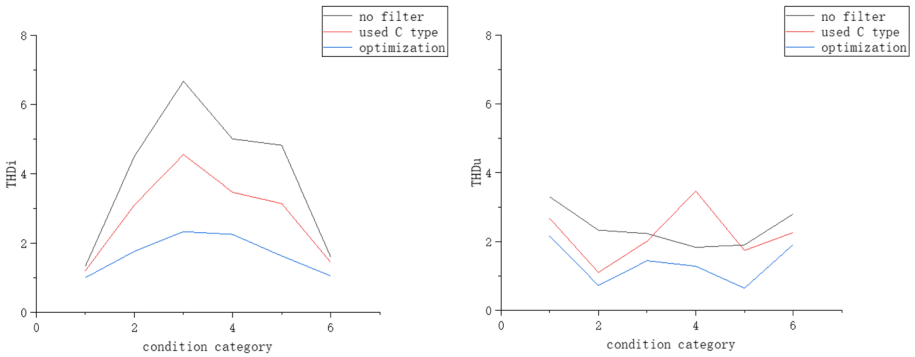

Fig. 18 Comparison of the total harmonic distortion rate of the current and voltage of the no filter, the used C type, and optimization

Table 6 Comparison before and after filtering

Condition category	THDi/THDu No filter	THDi/THDu Used C type	THDi/THDu Optimization
1	1.34/3.31	1.21/2.68	1.01/2.17
2	4.51/2.34	3.11/1.11	1.77/0.73
3	6.68/2.24	4.56/2.02	2.34/1.45
4	5.01/1.84	3.48/1.75	2.26/1.29
5	4.83/1.91	3.15/1.17	1.64/0.65
6	1.61/2.81	1.45/2.27	1.06/1.92

that the harmonic content is reduced to 1.77%, 0.73%, and 1.17%, respectively, after parameter optimization. Experiments show that the existence of filter impedance will lead to increase the negative sequence. After optimizing the parameters, the negative sequence problem can be compensated to a certain extent. Next, the filtering of voltage waveforms is shown.

As shown in Fig. 17, the above waveform results show that the voltage waveform is smoother, and the harmonic content is lower after the filter is added. Next, compare the voltage level and harmonics of the AT. Finally, the filtering results for all cases are summarized as follows.

As shown in Fig. 18 and the Table 6, regardless of the operating conditions, THDi and YHDu are clearly optimized to produce substantial improvements.

Conclusions

In this paper, the simulation model of locomotive harmonic source is established firstly. Combined with the parameters of a traction substation in China, the simulation of multi-condition locomotive operation is carried out, and the negative sequence and harmonic conditions of different working conditions are studied and analyzed respectively.

1. Based on the simulation design, the accurate optimization parameters of C-type filter under regenerative braking are obtained.

2. The optimized parameter design scheme balances the influence of existing filtering methods on negative sequence to some extent.
3. The filtering results of six operating conditions show that this method has low cost and high efficiency and is suitable for multiple operating conditions. It has a good application prospect in harmonic control of high voltage and high current occasions.

Abbreviations

TS	Traction substation
THD	Total harmonic distortion
TPSS	Traction power supply system
SVC	Static var compensator
STATCOM	Static synchronous compensator
RPC	Railway static power conditioner
FC	Full compensation
APF	Active power filter
PPF	Passive polyphase filter

Acknowledgements
Not applicable

Authors' contributions
HGZ as the supervision in this paper, HQZ and SZ gave the writing guide, DCZ and ZZW for the proofreading, JPZ and BLW provided data analysis, and JBZ review the grammar. All authors have read and approved the manuscript.

Funding
This work was supported in parts by the project of local colleges and universities capacity construction of Shanghai Municipal Science and Technology Commission (No. 20090503100) and the Science and Technology Innovation Action Plan "the Belt and Road" China Laos Railway Engineering International Joint Laboratory (21210750300).

Availability of data and materials
The data used to support the findings of this study are available from the corresponding author upon request.

Declarations

Competing interests
The authors declare that they have no competing interests.

Received: 16 August 2023 Accepted: 14 November 2023
Published online: 20 December 2023

References

1. Ming He, Chong Wang, Li Niu (2018) Impact of high speed railway traction power supply system on power quality of regional power grid. Electr Appl 37(23):52–57+73
2. Geng Hong, Xianyong Xiao, Junyong Liu (2003) Research and technical progress on power quality problems (1) - general concept of power quality. Power Autom Equip 10:1–4
3. Li Chao. (2020) Measured data management and data analysis of power quality in electrified railway. Beijing Jiaotong University
4. ZHANG Kai. (2020) A study on the utilization of regenerative braking energy of trains under the condition of traction power station. Southwest Jiaotong University
5. Pei Luo, Weimin Yang, Min Zhang (2018) Optimization of negative sequence current in public power grid under regenerative braking condition of high-speed railway. China Railway Sci 39(06):126–132
6. Zhang Min. (2012) Harmonic and negative sequence analysis of high-speed railway traction power supply system under regenerative braking condition. Southwest Jiaotong University
7. Tang Ji.Power quality analysis of high-speed railway traction power supply system. Zhengzhou University, 2016
8. Wang Bin. (2015) Power quality analysis of high-speed railway traction power supply system under regenerative braking condition. Southwest Jiaotong University
9. Wu H, Zeng L, Ren Q, Ai L (2022) Robust design scheme of C-type filter considering harmonic dynamic characteristics of traction power supply system. IEEE Access 10:47782–47791
10. Xie S, Zhang Y, Wang H (2021) A novel co-phase power supply system for electrified railway based on V type connection traction transformer. Energies 14(4):1214
11. Wang H, Liu Y, Yan K, Fu Y, Zhang C (2015) Analysis of static VAr compensators installed in different positions in electric railways. IET Electr Syst Transp 5(3):129–134
12. Rodrigues, P., Morais, V.A., Martins, A., Carvalho, A. (2019) STATCOM simulation models for analysis of electrified railways. In: 45th Annual Conference of the IEEE Industrial Electronics Society (IECON), Lisbon, Portugal, pp. 2257–2262

13. Mongkoldee K, Kulworawanichpong T (2021) Optimal sizing of AC railway power conditioner in autotransformer-fed railway power supply system. Int J Electr Power Energy Syst 127:106628
14. Wu C, Luo A, Shen J, Ma FJ, Peng S (2012) A negative sequence compensation method based on a two-phase three-wire converter for a high-speed railway traction power supply system. IEEE Trans Power Electron 27(2):706–717
15. Roudsari HM, Jalilian A, Jamali S (2019) Hybrid railway power quality conditioner based on half-bridge converter and asymmetric balanced tractiontransformer with deadbeat current control. IET Power Electron 12(13):3447–3459
16. Tamaskani Rohollah. (2022) Optimal design of C-type filter in harmonics polluted distribution systems. Energies,15(4)
17. Dai NY, Lao KW, Lam CS (2015) Hybrid railway power conditioner with partial compensation for converter rating reduction. IEEE Trans Ind Appl 51(5):4130–4138
18. Roudsari HM, Jalilian A, Jamali S (2018) Flexible fractional compensating mode for railway static power conditioner in a V/v traction power supply system. IEEE Trans Ind Electron 65(10):7963–7974
19. Dai NY, Lao KW, Wong MC, Wong CK (2012) Hybrid power quality conditioner for co-phase power supply system in electrified railway. IET Power Electron 5(7):1084–1094
20. Habibolahzadeh, M., Roudsari, H.M., Jalilian, A., Jamali, S. (2019) Hybrid SVCHPQC scheme with partial compensation technique in co-phase electric railway system. In: 27th Iranian Conference on Electrical Engineering (ICEE), Yazd, Iran, pp. 679–684
21. Hu H, Shao Y, Tang L, Ma J, He Z, Gao S (2018) Overview of harmonic and resonance in railway electrification systems. IEEE Trans Ind Appl 54(5):5227–5245
22. Wang Y, Xu S, Xu W, Wu J, Xiao X (2020) Comparative studies on design methods for detuned C-type filter. IEEE Trans Power Deliv 35(4):1725–1734
23. Xu W, Ding T, Li X, Liang H (2016) Resonance-free shunt capacitors—configurations, design methods and comparative analysis. IEEE Trans Power Deliv 31(5):2287–2295
24. Lange AG, Redlarski G (2020) Selection of C-type filters for reactive power compensation and filtration of higher harmonics injected into the transmission system by arc furnaces. Energies 13(9):2330
25. Jiang J (1999) Introduction to the national standard GB/T14549-93 "power quality utility grid harmonics"[J]. Power capacitors (02):23-27
26. Runda Lin, Yang Yu, Yong Wang, Zhicheng Deng (2018) Application and implementation of instantaneous symmetrical component method in negative sequence current detection. Measure Control Technol 37(10):49–53+59
27. Hu H. T (2014) Harmonic propagation and resonance analysis for tractionpower supply system of high-speed railway. Ph.D. dissertation, Dept. Elect. Eng., Southwest Jiaotong Univ., Chengdu

Publisher's Note